Rheological Behavior of Pure Binary Ni-Nb Model Alloys

David Piot, Frank Montheillet, S.L Semiatin

Rheological Behavior of Pure Binary Ni–Nb Model Alloys

David Piot[1,a], Frank Montheillet[1,b] and S. Lee Semiatin[2,c]

[1]École nationale supérieure des mines de Saint-Étienne, Centre SMS; CNRS UMR 5146
158 cours Fauriel, F–42023 ST ETIENNE CEDEX 2, FRANCE

[2]Air Force Research Laboratory, AFRL/RX, Wright-Patterson Air Force Base, OH 45433-7817, USA

[a]PIOT@EMSE.fr, [b]MONTHEIL@EMSE.fr, [c]Lee.SEMIATIN@WPAFB.AF.mil

Keywords: Superalloys, Rheology, Dynamic Recrystallization, Torsion Tests, Strain Hardening, Dynamic Recovery, Ni–Nb Alloys, Hot Working.

Abstract. This experimental work deals with the influence of niobium additions to high purity nickel on dynamic recrystallization behavior during hot working. Various high-purity alloys were prepared (unalloyed Ni and Ni–0.01, 0.1, 1 and 10 wt % Nb) and deformed to high strains by hot torsion tests to characterize the rheological behavior within the range 800 – 1000°C at strain rates of 0.03, 0.1 and 0.3 s^{-1}. Niobium additions strongly increased the flow stress. To quantify such behavior, the strain-hardening parameter h and dynamic-recovery parameter r in the Yoshie-Laasraoui-Jonas constitutive equation were determined from the initial part of the experimental stress-strain curves (*i.e.*, at strains before the stress peak) in which dynamic recrystallization does not alter the mechanical behavior. A table showing the variation of h and r as a function of strain rate, temperature, and niobium content was compiled and used to fit a simple empirical model for predicting h and r from the deformation conditions and alloy composition. In addition, microstructures were determined by optical metallography and SEM/EBSD. Based on this work, it appears that niobium additions noticeably refine the steady-state grain size by considerably decreasing the kinetics of dynamic recrystallization in nickel.

Introduction

Refining the grain size plays a central role in improving the mechanical properties of superalloys, One of the main ways to control grain size is *via* thermomechanical processing (TMP). The TMP of superalloys has been investigated to a far less extent than in steels. Nevertheless, discontinuous dynamic recrystallization (DDRX) is an important physical phenomenon contributing to the evolution of grain size in both material classes. The mechanism of DDRX is complex. It depends on the rheology of the material (strain hardening and dynamic recovery) and involves the nucleation of new grains and the migration of grain boundaries as well.

A new model of DDRX model has recently been developed, but it does not explicitly account for alloying effects such as solute drag or Zener pinning on boundary mobility [1]. To this end, the present work summarizes an experimental investigation of the mechanical behavior of *solid-solution* nickel alloys during hot working which was undertaken as a first step in the modeling of DDRX in alloys with solutes and precipitates. In particular, hot torsion tests were performed on high-purity binary nickel-niobium model alloys (due to the large range of solubility of Nb in Ni) to quantify the influence of such solute additions on strain hardening and dynamic recovery.

Materials and Procedures

Commercial superalloys have a complicated metallurgy and contain a large number of alloying elements. To avoid complex interactions, therefore, the present work focused on pure binary alloys, specifically pure nickel and four Ni–Nb alloys, *i.e.*, Ni – 0.01, 0.1, 1 and 10 wt % Nb. High-purity nickel was obtained by repeated induction melting of commercial (electrolytic-purity) material in a water-cooled silver crucible under a high-purity argon-hydrogen atmosphere. The alloys were

obtained by adding commercial-purity niobium (99.9 %) to the melt in the silver crucible. An ingot of ~1.1 kg was prepared for each alloy. The chemical compositions are summarized in Table 1.

Table 1. Chemical composition of program alloys (balance = Ni)

Alloy	Nb (wt %)	Fe (wt ppm)	C (wt ppm)	S (wt ppm)	O (wt ppm)	N (wt ppm)
Ni		150	5	<5	6	<5
Ni–0.01% Nb	0.0105		5.5	5	4.5	1
Ni–0.1 % Nb	0.07 – 0.09		4		7	
Ni–1% Nb	0.7 – 0.8		6		5	
Ni–10% Nb	9.5		6	5	3	3

Each ingot was hot forged and swaged at ~1050°C into a cylindrical bar of 10.7 mm diameter. Thirteen torsion specimens with a 6-mm diameter and 27-mm gauge length were machined from each bar for mechanical testing. All specimens were homogenized for 1 h at 700°C. Such an intermediate temperature was chosen to restrict grain growth. Microstructural investigations confirmed that the homogenization treatment had a negligible effect on grain size (close to 500 μm for Ni and Ni – 0.1 Nb and in the range of 50 – 100 μm for Ni – 1 Nb). According to the binary Ni–Nb phase diagram, niobium was in solid solution for the entire range of compositions in this work.

To quantify the plastic flow of the program materials, hot torsion tests were performed with an electromechanical, computer-controlled machine equipped with a furnace and gas-quenching device (providing a cooling rate ~100°C/s) which is automatically trigged at the desired final strain; the final strain in the present tests was 5, at which steady-state flow had been reached. Specimens were heated to tested temperature and stabilized ~15 min prior straining. The experimental conditions (Table 2) were carefully chosen (in light of the limited quantity of test material) to enable the determination of the strain-rate sensitivity of the flow stress at 800°C, 900°C and 1000°C and the apparent activation energy at 0.1 s^{-1}. There was only one exception; a torsion test at 1000°C and 0.03 s^{-1} was not conducted for pure nickel. Stress-strain curves were derived from the measured torque-twist data using the standard Fields-and-Backofen procedure.

Table 2. Experimental matrix for torsion tests

$\dot{\bar{\varepsilon}}$ \ T	800°C	850°C	900°C	950°C	1000°C
0.03 s^{-1}	×		×		×
0.10 s^{-1}	×	×	×	×	×
0.30 s^{-1}	×		×		×

Results and Discussion

The overall stress levels and the exact shape of the stress-strain curves depended on niobium content. Typical stress-strain curves are given in Fig. 1 for the case of pure nickel strained at 0.1 s^{-1} and various temperatures. For all the alloys, the flow curves exhibited a single peak, flow softening due to DDRX, and a steady-state regime (characterized by a constant stress) at larger strains. The steady-state condition was reached at an effective surface strain of ~0.5 – 1 in pure nickel, 1 – 1.5 in Ni –0.01 Nb, 1.5 – 2.5 in Ni – 0.1 Nb, or 3 – 4 in Ni –1 Nb and Ni – 10 Nb. The steady-state stress was in the range of 40 – 80 MPa for pure nickel, 50 – 110 MPa for Ni – 0.01 Nb, 60 – 150 MPa for Ni –0.1 Nb, 100 – 250 MPa for Ni – 1 Nb, and 200 – 400 MPa for Ni – 10 Nb.

The key rheological parameters, consisting of the strain-rate sensitivity and the apparent activation energy, were determined from the stress-strain curves.

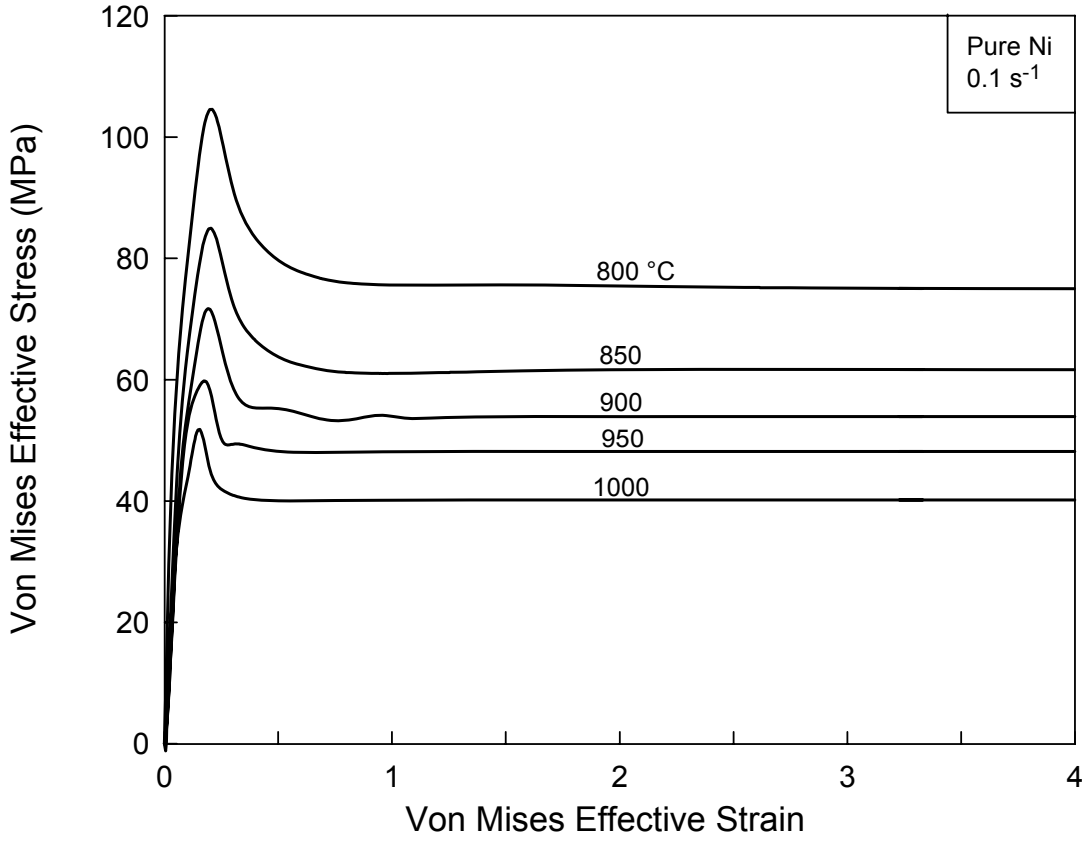

Figure 1. Stress-strain curves for pure nickel strained at 0.1 s^{-1} and various temperatures

Strain-Rate Sensitivity. The strain-rate sensitivity of the stress at 800, 900 and 1000°C was determined for both the peak (maximum) stress (m_m, Table 3) and the steady-state stress (m_s, Table 4) using $\log\bar{\sigma} - \log\dot{\bar{\varepsilon}}$ curves for each alloy. In all such plots, the points fell on a straight line, thus indicating that the rate sensitivities did not depend on strain rate *per se*.

Table 3. Strain-rate sensitivity of the peak stress, m_m

T \ Alloy	Ni	Ni–0.01 Nb	Ni–0.1 Nb	Ni–1 Nb	Ni–10 Nb
800°C	0.203	0.163	0.096	0.110	0.05
900°C	0.198	0.190	0.140	0.113	0.127
1000°C	0.143	0.165	0.167	0.142	0.179

Table 4. Strain-rate sensitivity of the steady-state stress, m_s

T \ Alloy	Ni	Ni–0.01 Nb	Ni–0.1 Nb	Ni–1 Nb	Ni–10 Nb
800°C	0.131	0.114	0.081	0.156	–
900°C	0.153	0.142	0.110	0.100	0.118
1000°C	0.149	0.145	0.137	0.107	0.111

In general, m_m was greater than m_s and, usually but not always, the values of m increased with temperature and decreased with niobium content. Furthermore, they were much smaller for dilute alloys than for pure nickel, but the tendency was unclear for high niobium contents.

Apparent Activation Energy. Apparent activation energies of hot deformation were derived for both the peak (Q_m) and steady-state (Q_s) stresses from plots of $\ln\bar{\sigma} - 1/T$ at a strain rate of 0.1 s^{-1} (Fig. 2). These plots were linear indicating that the product mQ did not vary with temperature, *per* the standard analysis of the strain-rate and temperature dependence of the flow stress.

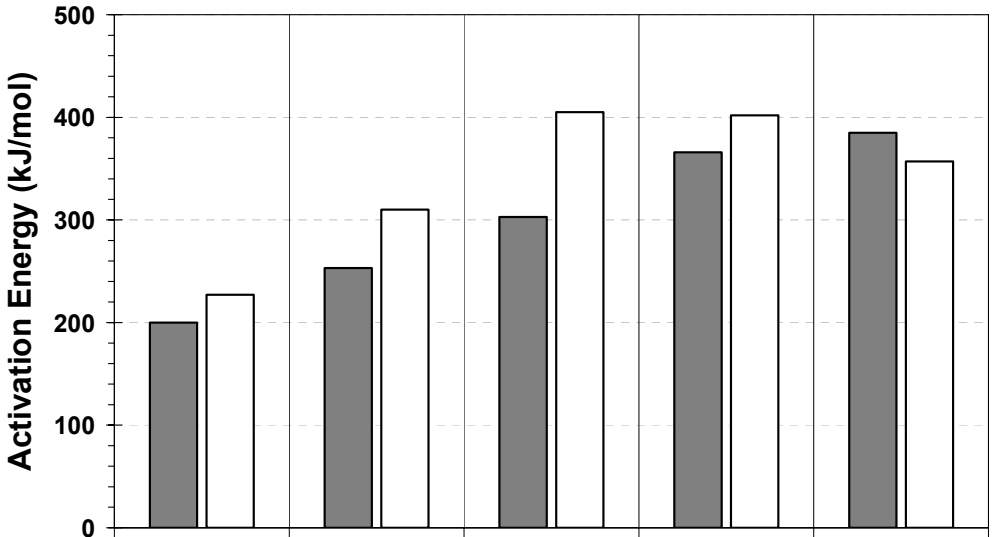

Figure 2. Apparent activation energy (in kJ/mol) of the peak stress (Q_m, gray bars) and steady-state stress (Q_s, white bars) for a strain rate of 0.1 s^{-1}

The apparent activation energy was greater for the steady-state stress (Q_s) compared to that for the peak stress (Q_m), except for Ni – 10 Nb. In addition, both activation energies increased with niobium content, at least for the dilute alloys (Nb ≤ 1 wt %).

Quantitative Analysis of Stress-Strain Curves. Each flow curve was analyzed using the Yoshie-Laasraoui-Jonas single-state-variable model describing strain hardening and dynamic recovery *prior to the onset of DDRX*, *i.e.*, $\mathrm{d}\rho/\mathrm{d}\varepsilon = h - r\rho$. Here, ρ is the dislocation density, h is the strain-hardening parameter, and r is the dynamic-recovery parameter. Combining this equation with the well-known relationship $\bar{\sigma} \propto \sqrt{\rho}$ and integrating, the following expression is obtained:

$$\bar{\sigma}^2 = \sigma_\infty^2 - \left(\sigma_\infty^2 - \sigma_e^2\right)\exp\left[-r\left(\varepsilon - \varepsilon_e\right)\right], \tag{1}$$

in which $\left(\varepsilon_e, \sigma_e\right)$ denotes the stress and strain at yielding, and σ_∞ represents the steady-state stress that would be achieved in the absence of DDRX. In the present research, the values of r and σ_∞ were determined from a best fit of the initial portions of the stress-strain curves; *i.e.*, for strains of $\varepsilon < (5/6)\varepsilon_m$ (ε_m = the strain at the peak stress), below which DDRX typically does not initiate. The h parameter was then derived from the equation $\sigma_\infty = \alpha\mu b\sqrt{h/r}$, in which b is the magnitude of the Burgers vector and μ is the elastic shear modulus (at the given test temperature). The values of h and r so determined are summarized in Table 5.

Analytical, closed-form expressions suitable for the modeling of DDRX (as described in a companion paper in this volume [1]) were derived to describe the dependence of h and r on strain rate, temperature, and niobium content. The relation for h was as follows:

$$h = h_0 \left(\frac{\dot{\varepsilon}}{\dot{\varepsilon}_0} \right)^{m_\mathrm{h}} \exp\left(\frac{m_\mathrm{h} Q_\mathrm{h}}{\mathrm{R}T} \right) \exp\left(A_0 \left(\frac{\dot{\varepsilon}}{\dot{\varepsilon}_0} \right)^{m_\mathrm{A}} \exp\left(\frac{Q_\mathrm{A}}{\mathrm{R}T} \right) \sqrt{c_\mathrm{m}} \right), \tag{2}$$

in which $A_0 = 0.236$, $\dot{\varepsilon}_0 = 0.1\,\mathrm{s}^{-1}$, $m_\mathrm{A} = -0.077$, $Q_\mathrm{A} = 17.1\,\mathrm{kJ.mol}^{-1}$, $h_0 = 2.42$ μm/μm^3, $m_\mathrm{h} = 0.14$, $Q_\mathrm{h} = 335\,\mathrm{kJ.mol}^{-1}$, and c_m is the niobium content (in wt %). The dynamic-recovery parameter r was described approximately by the expression $r = r_0 \exp(c_\mathrm{m} / c_0)$, in which r_0 and c_0 are strain-rate and temperature dependent. For instance, the temperature dependence at a strain rate of 0.1 s^{-1} is summarized in Table 6.

Table 5. Strain-hardening (h) and dynamic-recovery (r) parameters for Ni–Nb binary alloys at various temperatures and strain rates

$\dot{\varepsilon}$ (s^{-1})	θ (°C)	Nb (wt. %)	h (μm/μm^3)	r	$\dot{\varepsilon}$ (s^{-1})	θ (°C)	Nb (wt. %)	h (μm/μm^3)	r
0.03	800	0	493 (*)	10.1	0.1	800	0	414	3.5
		0.01	402	3.7			0.01	541	4.2
		0.1	708	5.2			0.1	771	4.4
		1	4199	13.3			1	5330	13.4
		10	106837	71.2			10	74570	42.5
	900	0	237	4.7		850	0	342	4.8
		0.01	291	5.9			0.01	483	5.1
		0.1	351	4.0			0.1	564	3.9
		1	1113	6.9			1	1871	6.6
		10	18447	34.0			10	N. A.	N. A.
	1000	0	N. A.	N. A.		900	0	303	7.0
		0.01	161	5.6			0.01	357	4.9
		0.1	223	5.5			0.1	454	4.0
		1	528	5.3			1	1262	5.6
		10	N. A.	N. A.			10	21289	28.4
0.3	800	0	448	2.4		950	0	451 (*)	19.1
		0.01	540	2.6			0.01	295	5.4
		0.1	799	4.0			0.1	330	3.7
		1	3224	7.6			1	1009	5.9
		10	40079	21.0			10	12600	22.6
	900	0	305	2.5		1000	0	201	8.3
		0.01	485	4.5			0.01	218	4.7
		0.1	527	3.5			0.1	258	3.7
		1	1512	5.5			1	776	6.1
		10	14621	13.7			10	12285	33.3
	1000	0	198	3.4					
		0.01	276	5.3					
		0.1	427	5.3					
		1	953	5.9					
		10	9162	16.4					

(*) not used

Table 6. Parameters for the prediction of r and their temperature dependence for a strain rate of 0.1 s^{-1}

Temperature	800°C	900°C	950°C	1000°C
r_0	5.72	4.47	4.59	4.36
c_0 (wt %)	4.84	5.40	6.25	4.89

Grain Size and the Derby Relationship. The average steady-state grain size at the surface of the deformed torsion specimens (at which $\bar{\varepsilon} = 5$), determined by optical metallography and (in selected instances) SEM/EBSD techniques, revealed that niobium alloying results in substantial grain refinement (Fig. 3). Furthermore, the slope of a log-log plot of flow stress versus grain size (*i.e.*, the so-called Derby exponent [2]) for each of the program alloys was compatible with classical values in the literature (*i.e.*, ~2/3). However, the overall fit (broken line in Fig. 3) yielded an exponent of ~1/3, which is somewhat smaller. It was also found, unexpectedly, that the steady-state stress decreased with increasing niobium content *for a given grain size*. The hardening effect of niobium in solid solution is thus likely related to grain refinement rather than to a direct solid-solution-strengthening effect.

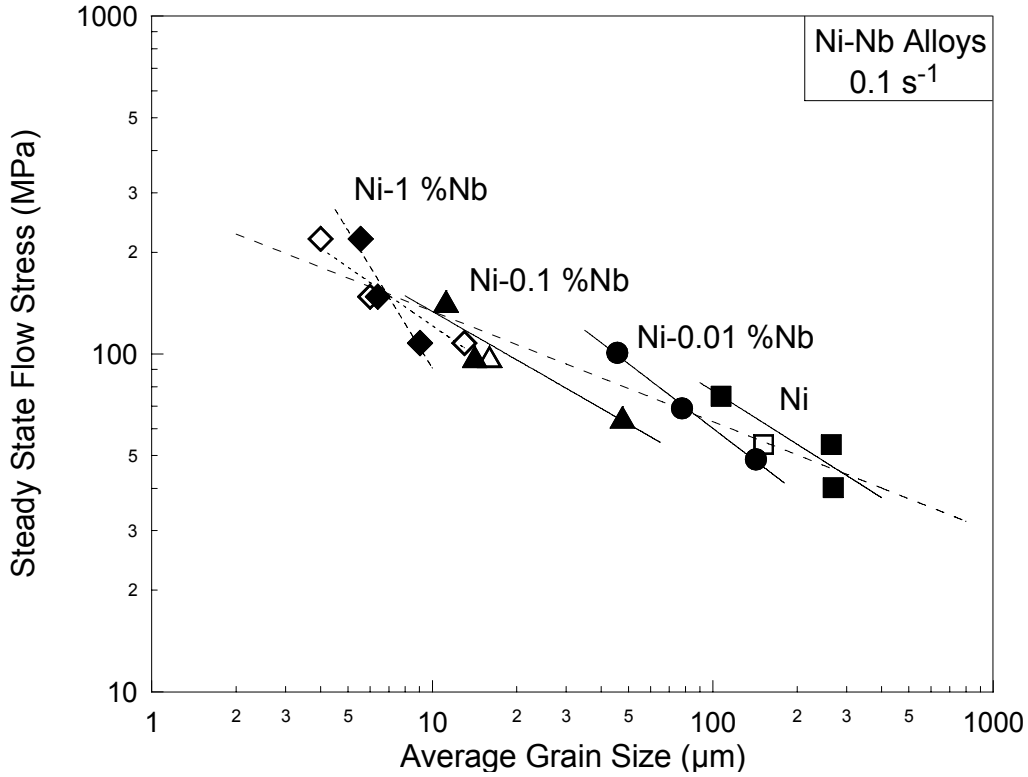

Figure 3. Derby relationship between flow stress and average steady-state grain-size. Grain sizes were determined by optical metallography (solid symbols) or SEM/EBSD (open symbols). The broken line is the best fit for all of the data determined from optical metallography.

References

[1] G. Damamme *et al.*: *A Model of Discontinuous DRX...* in the present proceedings.

[2] B. Derby: Scripta Metall. Vol. 27 (1992), p. 1581

Acknowledgment. This work was supported by the European Office of Aerospace Research & Development (EOARD) under contracts No FA8655-03-M-4061 and No FA8655-06-M-4001. The support and encouragement of the Air Force Office of Scientific Research (Dr. Joan Fuller, Program Manager) is also greatly appreciated.